Structure-function analysis of human l-prostaglandin D synthase bound with fatty acid molecules

Yangyan Zhou,*,†,[1] Neil Shaw,*,[1] Yang Li,* Yu Zhao,* Rongguang Zhang,* and Zhi-Jie Liu*,[2]

*National Laboratory of Biomacromolecules, Institute of Biophysics, Chinese Academy of Sciences, Beijing, China; and †Graduate University of Chinese Academy of Sciences, Beijing, China

ABSTRACT **Human prostaglandin D synthase (L-PGDS) is a lipocalin-type enzyme involved in the metabolism of arachidonic acid and plays a key role in the regulation of sleep, allergy, pain sensation, and the development of male reproductive organs. Here, using a combination of crystallographic, biochemical, mutagenesis, and kinetic studies, we have gained insights into the mode of ligand binding by human L-PGDS and have identified residues involved in catalysis. Interestingly, structural evidence reveals that 2 molecules of fatty acids, one molecule each of oleic and palmitoleic acid, bind inside the β barrel. The oleic acid is buried and binds in a highly basic patch in proximity to the catalytically critical Cys65, mimicking the binding of prostaglandin H_2. The palmitoleic acid sits in a relatively neutral region with very few interactions with the protein. Mutating Met64, Leu79, Phe83, or Leu131 to alanine reduced the catalytic efficiency by almost 10-fold, while K59A and Y149A mutations enhanced the catalytic efficiency by >2-fold. Met64 seems to function as a kinetic clamp, pushing the thiol group of Cys65 close to the site of nucleophilic attack during catalysis.—Zhou, Y., Shaw, N., Li, Y., Zhao, Y., Zhang, R., Liu, Z.-J. Structure-function analysis of human l-prostaglandin D synthase bound with fatty acid molecules. *FASEB J.* 24, 4668–4677 (2010). www.fasebj.org**

Key Words: allergy · arachidonic acid · lipocalin

Prostaglandin D synthase (PGDS) is an enzyme involved in the metabolism of arachidonic acid and is responsible for the conversion of prostaglandin H_2 (PGH_2) to prostaglandin D_2 (PGD_2) (**Fig. 1**) (1). PGD_2 is further metabolized to prostanoids such as 13,14-dihydro-15-keto-PGD_2 (DK-PGD2), Δ^{12} PGD_2, Δ^{12} PGJ_2, 15-deoxy-$\Delta^{12,14}$ PGD_2, 15-deoxy-$\Delta^{12,14}$ PGJ_2, and 9α11β PGF_2 (2). The levels of PGD_2 and its metabolites are elevated during inflammation and have been shown to be responsible for the pathological symptoms associated with allergic diseases. In addition, PGD_2 has been implicated in the regulation of sleep (3), sensation of pain (4), and the development of male reproductive organs (5).

Two isoforms of PGDS exist in humans. The hemopoetic type, H-PGDS, requires glutathione for catalysis and is primarily found in the cytoplasm (6), whereas the lipocalin type, L-PGDS, does not require glutathione for catalysis and is found in the brain, heart, and testis (7).

L-PGDS is the only lipocalin that, in addition to transporting lipids, functions as an enzyme (8). As a lipocalin, L-PGDS has been shown to bind numerous ligands, such as retinoic acid (9), bile pigments (10), amyloid β peptides (11), and gangliosides (12) and has been postulated to assist their transport. Interestingly, none of these ligands are related to prostanoid metabolism. Therefore, the physiological ligand of L-PGDS in its role as a lipocalin and an enzyme participating in the breakdown of arachidonic acid could be different. Further, it is quite intriguing that among all the enzymes involved in the metabolism of prostonoids, L-PGDS is the only enzyme that has a lipocalin fold.

The NMR structure of mouse L-PGDS (13) and the crystal structure of its C65A mutant reveal compartmentalization of the active site (14). The upper compartment encompasses residues essential for catalysis, while the lower compartment consists of highly conserved residues similar to those seen in lipocalins involved in the trafficking of ligands. Reaction kinetics of mouse L-PGDS mutants and results of thiol modification experiments seem to suggest that the thiolate anion of Cys65 activated by hydroxyl groups of Ser43, Thr67, and Ser81 mounts a nucleophilic attack on the substrate (14). However, a binary complex of the mouse L-PGDS with its substrate to support the proposed mechanism is lacking. Further, PGDS is known to bind ligands of varying dimensions, the structural basis for which is unknown.

Here we report the structure of human L-PGDS in complex with oleic acid (OLA) and palmitoleic acid (PLM). The structure provides insights into the role of PGDS in the transport of long-chain fatty acids. Using the structure as a guide, critical residues for catalysis have been identified by alanine scanning mutagenesis coupled with functional assays and kinetic analysis.

[1] These authors contributed equally to this work.

[2] Correspondence: National Laboratory of Biomacromolecules, Institute of Biophysics, Chinese Academy of Sciences, Beijing 100101, China. E-mail: zjliu@ibp.ac.cn

doi: 10.1096/fj.10-164863

0892-6638/10/0024-4668 © FASEB

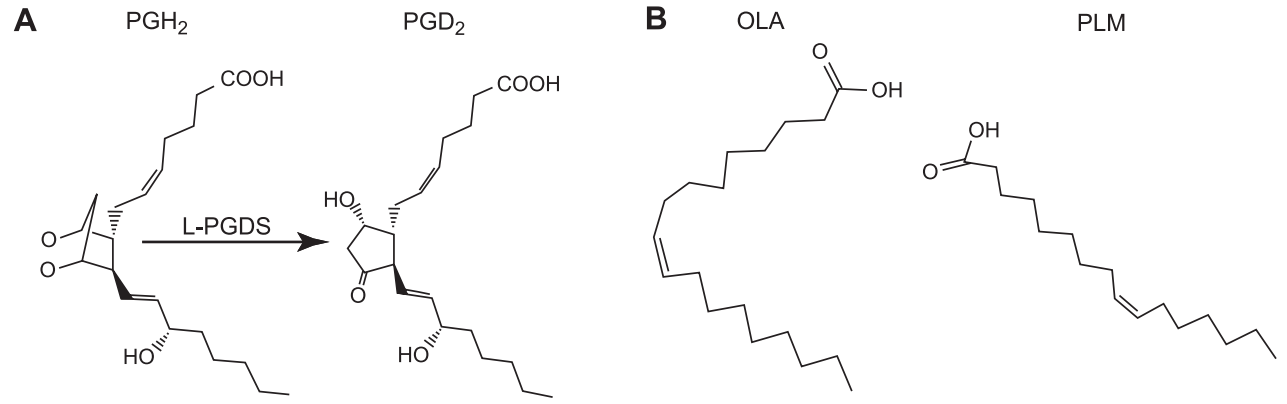

Figure 1. Reaction catalyzed by L-PGDS. *A*) L-PGDS converts PGH_2 to PGD_2. *B*) Chemical structure of OLA and PLM.

MATERIALS AND METHODS

Protein production

L-PGDS was amplified from the human brain cDNA library and cloned into a pMD-18T vector (Takara, Beijing, China). After verifying the DNA sequence, aa 29–190 were subcloned into pMCSG7 (15) for expression in *Escherichia coli* BL 21 (DE3). N-terminal hexa-His-tagged L-PGDS was produced by growing the cells in Luria-Bertani medium at 37°C for 4 h until $OD_{660\ nm}$ reached 0.8. Induction was carried out at 16°C for 20 h. Cells were harvested by centrifugation and lysed by sonication. Soluble L-PGDS was purified by Ni-affinity chromatography. After buffer exchange to remove the imidazole, His-tag was cleaved by treating the protein with tobacco etch virus (TEV) protease. Uncut protein and TEV were removed by a second round of Ni-affinity chromatography. The protein was exchanged into a buffer containing 20 mM Tris-HCl (pH 8.0), 200 mM NaCl, and 1 mM DTT using a Superdex G75 size-exclusion column. After concentration using 10-kDa-cutoff centrifugal concentrators, the protein (15–20 mg/ml) was immediately set up for crystallization.

Crystallization and data collection

Crystallization screening was carried out using commercially available sparse matrix screens. Here 1-μl hanging drops containing 0.5 μl protein mixed with 0.5 μl mother liquor were equilibrated over a 300-μl reservoir solution and incubated at 16°C. Crystals grown in 0.1 M citric acid (pH 4.0) and 1.7 M ammonium sulfate diffracted X-rays to 1.66 Å at beamline BL17U1 at the Shanghai Synchrotron Radiation Facility (SSRF; Shanghai, China). Similarly, 2 other crystal forms were obtained by varying the concentration of ammonium sulfate (**Table 1**).

Structure determination

Crystals were frozen in liquid nitrogen prior to diffraction testing and data collection. Native diffraction data were collected at a wavelength of 0.979 Å at beamline BL17U1 at SSRF. Data were indexed and scaled to 1.66-Å resolution using HKL2000. The structure was solved by the molecular replacement method using MolRep (16) with the structure of the mouse L-PGDS [Protein Data Bank (PDB) code 2CZU, chain A] as a search model. All the solvent molecules were removed prior to molecular replacement. The asymmetric unit consists of 1 molecule of human L-PGDS. PHENIX. AutoBuild (17) was used to rebuild the model with the initial phase. The model was manually improved in Coot (18). Refinement was carried out using REFMAC (19) and PHENIX (17) alternately. Structures of crystal forms 2 and 3 were solved by using the structure of crystal form 1 as the search model. Details of data collection and refinement statistics are listed in Table 1. The quality of the final model was validated with MOLPROBITY (20).

L-PGDS assay

Human L-PGDS was assayed as described previously (5), but with slight modifications. Briefly, a 50 μl reaction mixture containing enzyme mixed with 40 μM PGH_2 in 100 mM Tris-HCl (pH 8.0), 100 mM NaCl, and 1 mM DTT was incubated at 25°C for 1 min. At the end of the incubation period, the reaction was stopped by the addition of 50 μl acetone. The amount of product PGD_2 formed was estimated using the commercially available PGD_2-MOX ELISA kit (Cayman Chemicals, Ann Arbor, MI, USA). One unit of enzyme activity is defined as the amount of PGD_2 formed per minute under the assay conditions.

Gas chromatography/mass spectrometry (GC/MS) analysis

GC/MS analysis was performed at the Analysis Center of the Institute of Zoology, Chinese Academy of Sciences (Beijing, China). Briefly, the ligand was extracted from the purified protein using a mixture of chloroform and methanol (2:1 v/v) and derivatized to its methyl ester form by treatment with methanolic HCl. The derivatized sample was analyzed on a DSQ instrument (Thermo Finnegan, San Jose, CA, USA) equipped with an EI detector. Analytes were separated using a 30-m × 0.25-mm × 0.25-μm AB-5MS chromatographic column (Abel Industries, Pitt Meadows, BC, Canada) and were injected directly into the ion source of the MS. Helium was used as the carrier gas with a flow rate of 1 ml/min, and the column pressure was maintained at 100 kPa throughout the experiment. The temperature of the split/splitless injector was set to 280°C. The GC oven was programmed as follows: initial temperature, 80°C for 20 s; ramp up from 80 to 240°C at 4°C/min; hold at 240°C for 10 min. The sample was injected in 30:1 split mode at the rate of 1 ml/min. The GC/MS interface and the ion trap temperature were set at 280 and 200°C, respectively. The energy of the EI source of the mass spectrometer was set to 70 eV. Full-scan chromatograms were recorded by scanning from 50 to 410 m/z.

Site-directed mutagenesis

Amino acids were mutated to alanine using the Quick Change™ site-directed mutagenesis kit (Stratagene, La Jolla, CA, USA) follow-

TABLE 1. *Data collection and refinement statistics*

Statistic	Native C65A L-PGDS		
	Crystal form 1	Crystal form 2	Crystal form 3
Data collection	BL17U1, SSRF	BL17U1, SSRF	BL17U1, SSRF
Wavelength (Å)	0.9794	0.9794	0.9794
Space group	$P6_122$	$P4_1$	$P6_122$
Cell dimensions			
a, *b*, *c* (Å)	60.51, 60.51, 177.23	90.22, 90.22, 35.64	60.97,60.97, 179.46
α, β, γ (deg)	90.0, 90.0, 120.0	90.0, 90.0, 90.0	90.0, 90.0, 120.0
Resolution (Å)	20.0–1.66	50.0–1.70	50.0–1.40
R_{sym}	0.067 (0.389)	0.050 (0.322)	0.060 (0.302)
$I/\sigma I$	58.59 (4.56)	34.46 (1.74)	68.34 (4.32)
Completeness (%)	97.7 (84.5)	92.8 (63.0)	99.9 (100.0)
Redundancy	15.8 (6.8)	6.4 (3.5)	20.6 (11.8)
Refinement			
Resolution (Å)	19.60–1.66 (1.73–1.66)	90.22–1.70 (1.76–1.70)	30.49–1.45 (1.45–1.40)
Reflections	23,089 (2349)	28,122 (1668)	39,672 (3719)
R_{work}/R_{free}	17.83/24.38 (16.06/28.95)	19.88/26.10 (21.90/26.36)	19.44/22.05 (17.08/18.68)
Atoms			
Protein	1280	2747	1397
Ligand	1 OLA 1 PLM	1 OLA 1 PLM	1 OLA 1 PLM
Water	171	157	200
RMS deviations			
Bond lengths (Å)	0.010	0.012	0.005
Bond angles (deg)	1.423	1.452	0.989
Mean *B* value (Å^2)	23.00	16.07	17.89
Ramachandran analysis			
Favored region (%)	146 (97.33)	299 (95.53)	120 (98.36)
Allowed region (%)	3 (2.00)	8 (2.56)	1 (0.82)
Outliers (%)	1 (0.67)	4 (1.28)	1 (0.82)

Numbers in parentheses are statistics for the highest-resolution shell.

ing the manufacturer's instructions. All the clones were sequenced to confirm the mutation prior to expression.

Accession codes

The atomic coordinates and structure factors of crystal forms 1–3 of human L-PDGS have been deposited in the Protein Data Bank under accession codes 3O19, 3O2Y, and 3O22, respectively.

RESULTS

Human L-PGDS expressed in *E. coli* did not crystallize. Therefore, we mutated the putative catalytic nucleophile Cys65 to alanine to aid the crystallization of human L-PGDS. The mouse L-PGDS was crystallized using a similar strategy (14). The C65A mutant of human L-PGDS produced crystals that diffracted X-rays to 1.66-Å resolution. The structure was solved by molecular replacement using the structure of mouse L-PGDS (PDB code 2CZU, chain A) as a template. Residues Ser109–Gly113 could not be traced because of poor electron density. Interestingly, we observed a long stretch of unknown electron density embedded inside the β barrel. The density may have originated from a ligand bound by human L-PGDS during its expression in *E. coli*. Since the extra density exhibited clear nonsolvent electron density and was for the most part tubular, indicating the presence of a long aliphatic carbon chain, the initial interpretation was that the unknown density represented a fatty acid. The ligand was extracted from the protein using a mixture of chloroform and methanol (2:1 v/v) and subjected to a GC/MS analysis. Interestingly, the analysis indicated the presence of OLA and PLM, suggesting that the L-PGDS may have bound 2 different molecules of fatty acid. One molecule of *cis*-OLA could be fitted into the U-shaped electron density, while a *cis*-PLM could be modeled into the adjacent, slightly curved density. The omit electron density map suggested that the PLM seems to assume 2 conformations. The ω carbon is buried further deep inside the β barrel by 3.3 Å in the alternative conformation. The position of the ω carbon of PLM in the alternative conformation, which has an occupancy of 0.45, obstructs the placement of the ω carbon of OLA. As a result, the aliphatic tail of OLA is displaced vertically upwards toward the surface by 8.9 Å. These alternative conformations of OLA have an occupancy of 0.45 and 0.55, respectively. The $2|F_o| - |F_c|$ electron density contoured at the 1.0-σ level unambiguously suggests 2 alternative conformations for the ligands.

Overall structure

Human L-PGDS crystallized under slightly different conditions showed subtle differences in structure (Table 1). All 3 crystal forms reported here bound the same ligands. Crystal form 1 contains a single molecule of L-PGDS in the asymmetric unit and displayed the best density for the ligands. Crystal form 2 contains a dimer of L-PGDS in the asymmetric unit. Interestingly, the analytical ultracentrifugation results suggest that the wild-type and C65A mutant of human L-PGDS exist as a monomer in solution. The dimerization might have occurred because of crystal packing preferences. Crystal form 3 diffracted the best and displays an unusual conformation for the C65A, which has implications on the mechanism. The solvent content for crystal forms 1, 2, and 3 is 52.76, 38.98, and 54.04%, respectively. The overall structure of human L-PGDS reveals a typical lipocalin fold (**Fig. 2*A***) and closely mirrors the structure of mouse L-PGDS (PDB code 2CZU). Differences are observed in the positioning of helix α2 and the loop regions between strands E–F and G–H. These regions are in proximity of the ligand bound by human L-PGDS, and therefore the differences might have arisen because the mouse L-PGDS structure is without any ligand. Trp54 of the Ω loop and His111 from the E–F loop have been postulated to regulate access to the active site in mouse L-PGDS by forming an aromatic bridge. Most of the E–F loop (Ser109–Ser114 connecting strands E–F) is disordered in the structure of human L-PGDS bound with fatty acids. In addition, the position of Trp54 is different from that observed in mouse L-PGDS (14). To find out whether human L-PGDS uses Trp54 and His111 for the opening and closing of the active site similar to the mouse L-PGDS, several batches of L-PGDS were crystallized at slightly different conditions and used for data collection to map the location of the residues of the E–F loop. A different crystal form with the space group $P4_1$ yielded clear density for the residues Trp54 and His111 (Table 1). Interestingly, the side chains of Trp54 and Trp112 (not His111) are 3.5 Å apart and appear to be closing the active site (Fig. 2*B*). Trp112 is replaced by a serine in mouse L-PGDS. The location of the putative nucleophile, Cys65, in human L-PGDS is of particular interest and has implications for the mechanism of catalysis. Cys65, which was mutated to alanine, is seen sitting at the edge of strand B. Unlike the mouse L-PGDS, strand B in human C65A L-PGDS is twisted clockwise, and therefore the alanine is facing outside the cavity of the β barrel, suggesting that the side chain of Cys65 is oriented away from the cavity and toward the outside of the barrel (Fig. 2*A*). The N-terminal of human L-PGDS is seen capping the bottom of the β barrel. The position of the side chain of Phe34 is similar to that observed in the mouse L-PGDS. The side chain of Phe34 has been speculated to plug the bottom in the closed conformation of mouse L-PGDS, while a disordered Phe34 in the open conformation has led the authors to conclude that it unplugs the bottom of mouse L-PGDS in its open conformation. In contrast, the N-terminal region of human L-PGDS covering the bottom of the β barrel is well ordered, and Phe34, Phe44, and Gln36 are seen plugging the bottom. To unplug the bottom of the human L-PGDS, the entire loop region observed in the structure, Val29–Arg42, needs to move.

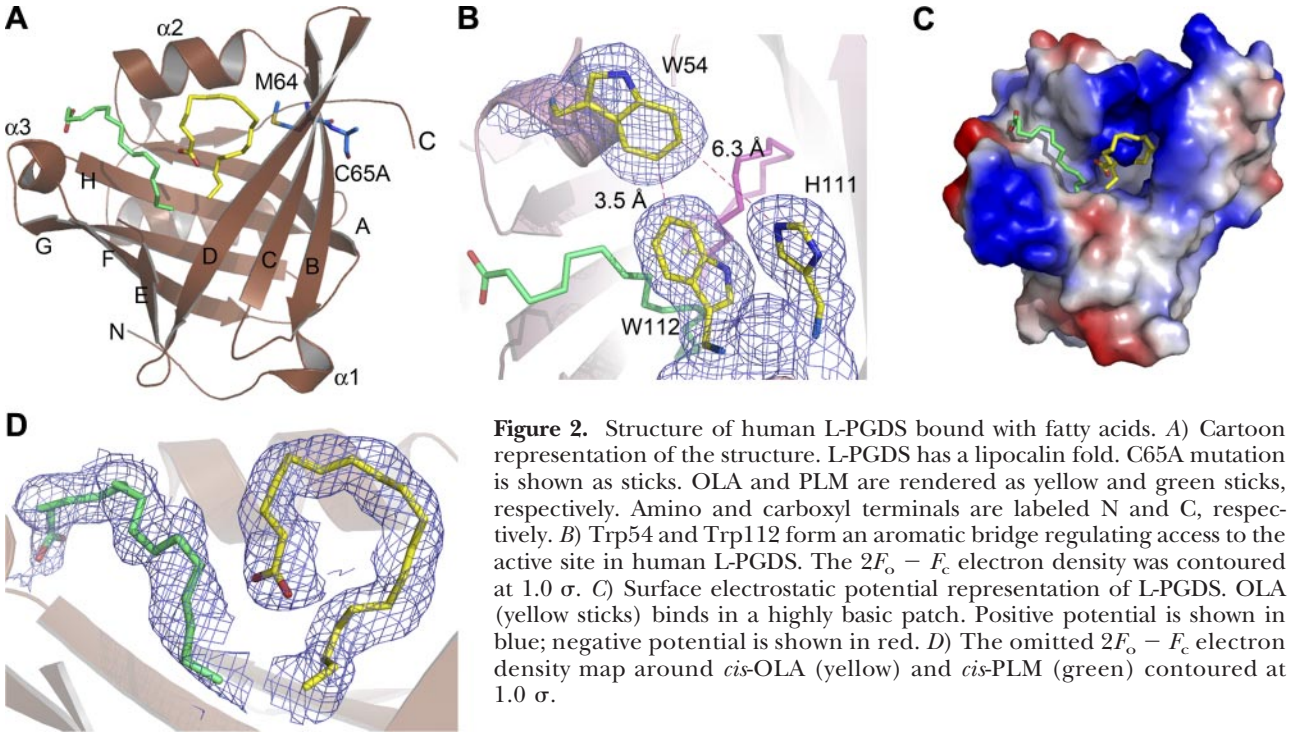

Figure 2. Structure of human L-PGDS bound with fatty acids. *A*) Cartoon representation of the structure. L-PGDS has a lipocalin fold. C65A mutation is shown as sticks. OLA and PLM are rendered as yellow and green sticks, respectively. Amino and carboxyl terminals are labeled N and C, respectively. *B*) Trp54 and Trp112 form an aromatic bridge regulating access to the active site in human L-PGDS. The $2F_o - F_c$ electron density was contoured at 1.0 σ. *C*) Surface electrostatic potential representation of L-PGDS. OLA (yellow sticks) binds in a highly basic patch. Positive potential is shown in blue; negative potential is shown in red. *D*) The omitted $2F_o - F_c$ electron density map around *cis*-OLA (yellow) and *cis*-PLM (green) contoured at 1.0 σ.

Fatty acid binding site

Two molecules of fatty acid bind inside the large cavity of the β barrel (Fig. 2). Based on the mode of binding of the fatty acid molecules, the cavity can be divided into 2 distinct regions. Site 1 is highly basic, partially buried, and 1 molecule of OLA binds in this region. On the other hand, site 2 is relatively neutral and extends to the surface of the cavity. One molecule of PLM binds in this region (Fig. 2*C*). Both the fatty acids seem to assume 2 conformations. The ω end of PLM is pushed deeper inside the β barrel in the alternative conformation, whereas that of OLA is displaced to the surface (**Fig. 3*A***). The aliphatic chain of OLA is seen partially encircling the side chain amine nitrogen of Lys 59, before getting buried deep inside the cavity (Figs. 3*A, B*). Both the carboxyl oxygen molecules of OLA are interacting with the amine nitrogen. This interaction probably localizes the fatty acid inside the cavity. Carbon atoms C1–C15 of the OLA are within van der Waal's distance of the amine nitrogen of Lys59, with C1, C2, C6, and C11–14 forming hydrogen bonds. In addition, the hydroxyl oxygen of Tyr149 is forming a hydrogen bond with the C17 of OLA. Tyr149, Ser67, and Leu79 form the lower edge of the binding site for OLA (Fig. 3*B*). The interaction of Met64 and Met94 with OLA is of interest. Met64 is adjacent to the putative nucleophile, Cys65. Although the side chain of Met64 is protruding inside the cavity, with the sulfur atom interacting with the carboxyl oxygen O2 of OLA (Fig. 3*B*), the side chain of Cys65 (mutated to alanine) is seen oriented toward the outside of the β barrel and in proximity to the disulfide bond formed between Cys167 and Cys186. Notably, Cys65 does not interact with the fatty acid ligand bound inside the cavity of the β barrel. The sulfhydryl group of Met94 is interacting with the carboxyl oxygen O1 of the ligand OLA. In contrast to OLA, the carboxyl oxygens of PLM are lying on the surface, while the ω carbon is buried deep inside the cavity. Interestingly, the carboxyl oxygens of PLM are not involved in any hydrogen bonding interactions and are seen engaged in only weak interactions with Ser52, Asn51, and Asp142. A tryptophan (Trp54), a tyrosine (Tyr116), a phenyl alanine (Phe143), and a leucine (Leu55) residue seem to guide and orient the aliphatic chain of PLM inside the cavity (Fig. 3*B*). In addition, side chains of Ser133 and Met94 interact with the aliphatic chain of PLM. Compared to OLA, the ligand molecule PLM has very few interactions with the protein, suggesting a weak binding mode.

A total of 171 water molecules were modeled in the structure. Some of the water molecules are buried inside the β barrel. Among the buried water molecules, the positions of Wat11, Wat48, and Wat99 are of interest, because they are interacting with OLA (Fig. 3*C*). Wat11 forms a 2.7- and a 2.6-Å hydrogen bond with the hydroxyl oxygens of Ser81 and Tyr149, respectively. On the other hand, Wat48 forms 2.8-Å hydrogen bonds with the hydroxyl oxygens of Ser45 and Ser67. Interestingly, Wat48 sits in the center of a triangular pocket formed by the hydroxyl oxygens of Ser45 and Ser67 and the thiol group of Cys65, when the structure of the unliganded L-PGDS (PDB code 2WWP) was superposed on our C65A mutant bound with fatty acids to map the location of Cys65 (Fig. 3*D*). Wat48 is hydrogen bonded to Wat99 *via* a 2.85-Å hydrogen bond. Wat99 is seen interacting with the C10 atom of OLA and Ser81. In addition, it is forming a 2.8-Å hydrogen bond with the sulfhydryl group of Met64. The proximity of these water molecules to OLA and the putative nucleophile Cys65 suggests a role for water molecules in catalysis.

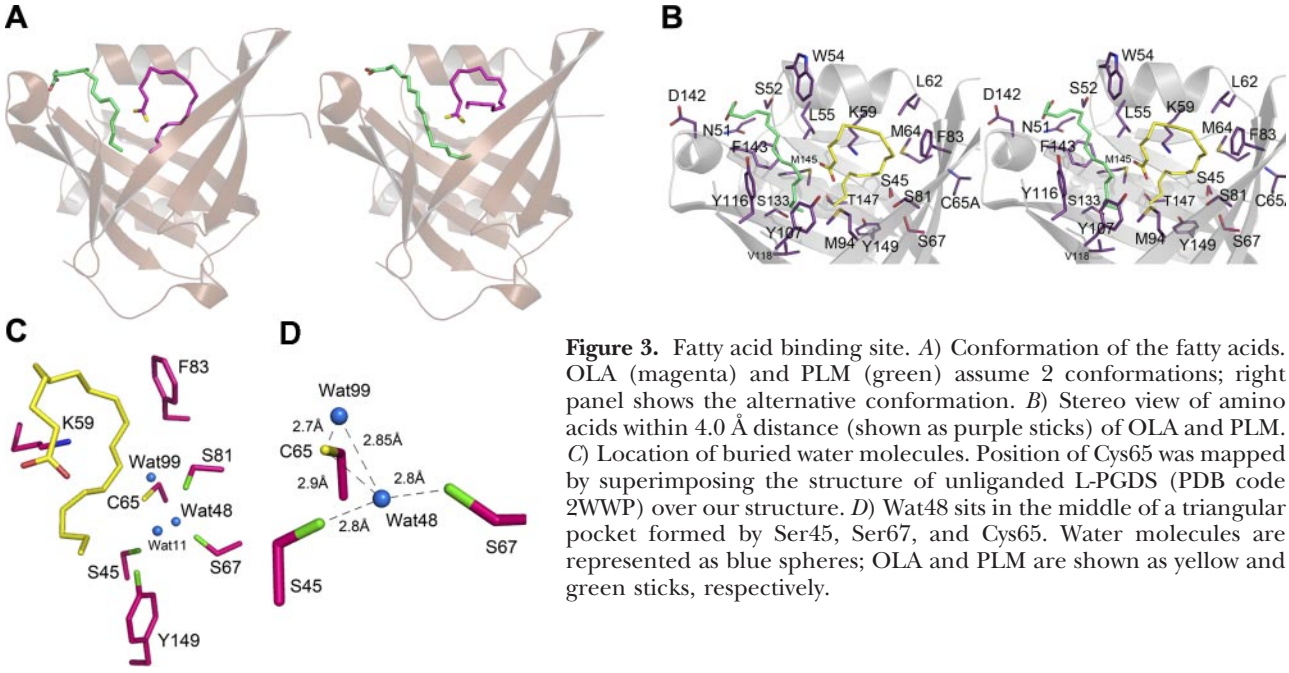

Figure 3. Fatty acid binding site. *A*) Conformation of the fatty acids. OLA (magenta) and PLM (green) assume 2 conformations; right panel shows the alternative conformation. *B*) Stereo view of amino acids within 4.0 Å distance (shown as purple sticks) of OLA and PLM. *C*) Location of buried water molecules. Position of Cys65 was mapped by superimposing the structure of unliganded L-PGDS (PDB code 2WWP) over our structure. *D*) Wat48 sits in the middle of a triangular pocket formed by Ser45, Ser67, and Cys65. Water molecules are represented as blue spheres; OLA and PLM are shown as yellow and green sticks, respectively.

TABLE 2. *Kinetic comparison between wild-type and mutant forms of human L-PGDS*

Mutation	K_m (μM)	V_{max} (μmol min^{-1} mg^{-1})	K_{cat} (s^{-1})	K_{cat}/K_m (s^{-1} μM^{-1})	Conservation of residue
Wild type	13.8	9.27	2.64	11.49	
C65A	–	0	–	–	Absolute
S45A	20.4	7.85	2.23	6.57	No
W54A	16.1	8.42	2.40	8.94	Absolute
K59A	12.3	17.84	5.84	24.84	Absolute
M64A	32.5	2.25	0.63	1.17	Absolute
L79A	32.8	0.215	0.06	0.11	Conserved
S81A	18.5	10.2	2.91	9.42	No
F83A	24.5	3.05	0.87	2.12	Highly
M94	20.2	7.88	2.24	6.66	No
L131A	25.2	2.80	0.81	1.89	Conserved
T147A	15.4	12.87	3.67	14.29	Conserved
Y149A	12.7	20.6	5.73	27.05	Highly

Alanine scanning mutagenesis and kinetic analysis

To find out which amino acids are important for catalysis, we carried out alanine scanning mutagenesis of residues surrounding the putative catalytic nucleophile Cys65. Because the OLA ligand binds in proximity of Cys65, potentially mimicking binding of the substrate, residues surrounding the OLA binding site were also mutated (**Table 2**). The findings have been extrapolated to other orthologs of L-PGDS by aligning the sequences obtained by running a PSI-BLAST search (21) for homologs of human L-PGDS (**Fig. 4**). Wild-type and mutant enzymes were expressed and purified to homogeneity using affinity and size exclusion chromatography. The purity of the proteins was confirmed by SDS-PAGE before carrying out the assays under identical conditions. As expected, C65A mutation abolished the enzymatic activity (Table 2). Previous studies of mouse L-PGDS have shown that a C65A mutation inactivates the enzyme (22). Cys65 occupies a similar position in the structures of human and mouse L-PGDS and is highly conserved among all the orthologs of L-PGDS, except in zebrafish, where a glycine occupies the position of the cysteine (Fig. 4). However, the L-PGDS from zebrafish has been shown to have no enzymatic activity (23). Mutating Ser45 or Ser81 to alanine decreased the catalytic efficiency by 43 and 18%, respectively. Both the mutations resulted in an increase in the K_m. Although the S45A mutation resulted in a decrease in V_{max}, the S81A mutation increased the V_{max} marginally (Table 2). The serines are located deep inside the β barrel close to the putative

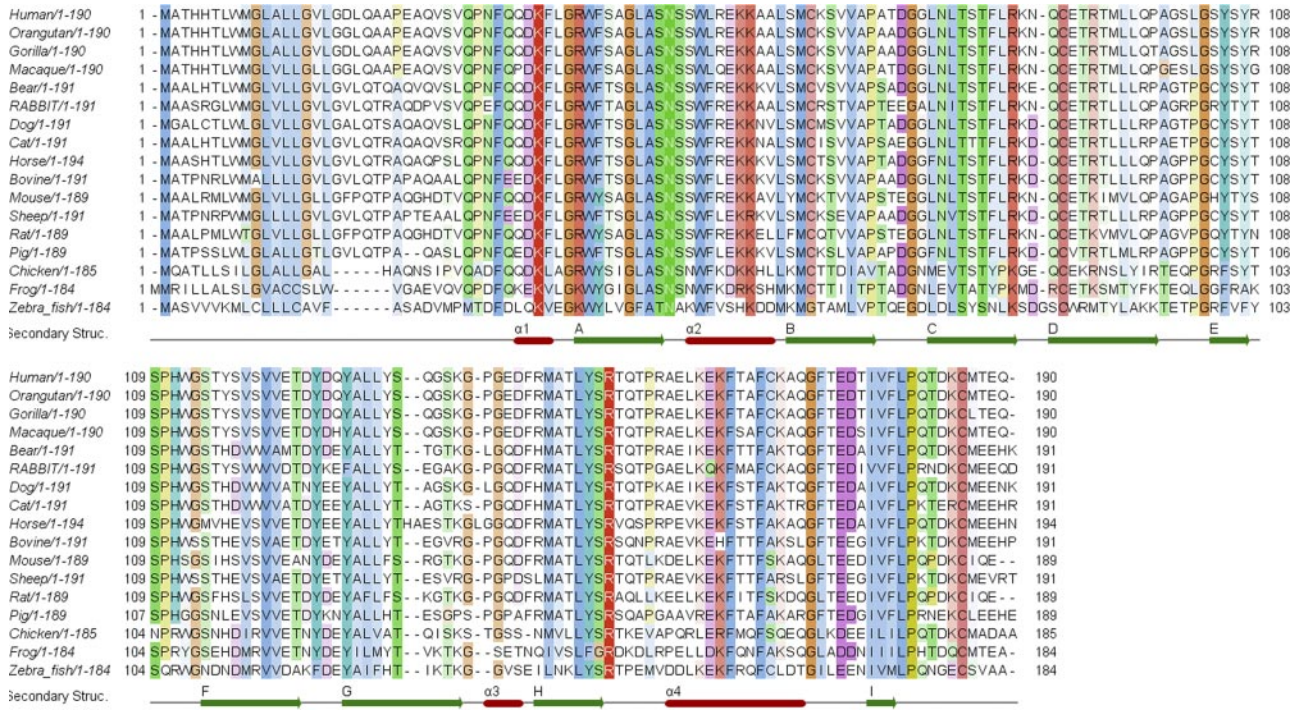

Figure 4. Sequence alignments of the orthologs of L-PGDS. Conservation is colored according to Clustal W convention. Secondary structure of human L-PGDS is annotated at bottom.

nucleophile Cys65. They have been postulated to assist the lowering of pKa of cysteine and stabilization of the thiolate ion (14). In the structure of human L-PGDS, Ser45 and Ser81 are in proximity to the OLA ligand, suggesting that they might interact with the substrate. In addition, the hydroxyl group of Ser81 has a weak interaction with the side chain of Tyr149, which forms the lower edge of the binding pocket. Ser45 is replaced by a threonine and a leucine in the bovine and zebrafish L-PGDS, respectively, whereas a tyrosine occupies the position of Ser81 in zebrafish. Trp54 is located on the surface and is part of the Ω loop covering the cavity of the β barrel (Fig. 2*B*). W54A mutation decreased the catalytic efficiency by 22%. Interestingly, K59A mutation almost doubled the V_{max} and increased the catalytic efficiency by 2-fold. In the structure of human L-PGDS, the aliphatic chain of the OLA ligand is seen forming numerous hydrogen bonds while encircling the amine nitrogen of Lys59. A K59A mutation probably helps accelerate product release. Although Trp54 and Lys59 are absolutely conserved among all the orthologs of L-PGDS, it seems that they may not be essential for catalysis; rather, given their surface location, they might play a role in imparting substrate specificity. Mutating Met64, Leu79, Phe83, or Leu131 to alanine decreased the catalytic efficiency by almost 10-fold (Table 2). Met64 and Phe83 are located inside the β barrel and are in proximity to Cys65 and the OLA ligand, suggesting that they might interact with the substrate PGH_2. Leu79 and Leu131 are buried deep inside the β barrel and together with Tyr149 seem to be forming the lower edge of the substrate binding site. Circular dichroism analysis of the M64A, L79A, F83A, and L131A mutants revealed no obvious differences in the secondary structural elements when compared to the wild-type enzyme. These amino acids seem to be critical for the binding and optimal orientation of the substrate during catalysis. Although Met64 is absolutely conserved, Phe83 is replaced by a tyrosine and an asparagine in chicken and zebrafish L-PGDS, respectively. An aromatic ring seems to be important for activity at the position of Phe83. Leu79 is highly conserved among all the orthologs, with an exception of another hydrophobic residue, valine, occupying the position of Leu79 in chicken L-PGDS. Leu131 is substituted by a phenylalanine and an isoleucine in the L-PGDS from rat and zebrafish, respectively. M94A mutation decreased the catalytic efficiency by almost half. In the structure of human L-PGDS the side chain of Met94 is seen protruding inside the β barrel and is interacting with the carboxyl oxygen of the OLA ligand, suggesting that Met94 might be involved in substrate binding. Met94 is not conserved among the orthologs of L-PGDS. T147A and Y149A mutations increased the catalytic efficiency of the enzyme. Although the increase in catalytic efficiency for T147A was marginal, Y149A increased the catalytic efficiency by almost 2.5-fold (Table 2). A modest change in K_m and a substantial increase in V_{max} and K_{cat} values seem to suggest that the catalytic efficiency of the mutants might have increased because of a faster product release. Thr147 and Tyr149 are buried deep inside the β barrel of human L-PGDS and interact with the aliphatic chain of OLA ligand, restricting any further downward movement of the ligand. Replacement of Tyr149 with alanine probably abolishes the hydrogen bonding interaction of the hydroxyl group with the substrate PGH_2, thereby hastening the exit of the product from the active site. Tyr149 is absolutely conserved in all the orthologs of L-PGDS (Fig. 4).

DISCUSSION

GC/MS analysis results showed that the wild-type and mutant C65A human L-PGDS consistently bound the same ligands when produced under conditions mentioned in methods. Attempts to remove the ligands resulted in precipitation of the protein. Therefore, the enzyme bound with the ligands was used for activity assays. The wild-type enzyme displayed a K_m of 13.8 μM and V_{max} of 9.27 μmol/min/mg protein when PGH_2 was used as a substrate, implying that the human L-PGDS produced in *E. coli* was active (Table 2). Further, the wild-type L-PGDS bound with fatty acids could catalyze the reaction when tested for activity. These observations suggest that the substrate PGH_2 probably has a higher affinity for the binding pocket than the fatty acids and displaces them from the active site during catalysis.

M64 acts as a kinetic clamp

Interestingly, in the structure of the C65A mutant of human L-PGDS bound with fatty acids, the side chain of M64 is pointing inside the β barrel, whereas the side chain of Cys65 (mutated to alanine) is oriented toward the outside of the β barrel (Figs. 2*A* and **5*A***). However, for the catalysis to occur, the side chain of Cys65 needs to point inside the β barrel. A recent structure of unliganded human L-PGDS deposited in PDB (accession code 2WWP) shows that the side chain of Cys65 is oriented inside the β barrel, whereas the side chain of Met64 is facing outside the β barrel (**Fig. 5*A***). Such a position for Cys65 and Met64 can be accomplished by twisting the strand B in an anticlockwise direction, as observed in 2WWP (Fig. 5*A*). Binding of the substrate PGH_2 inside the β barrel probably pushes the strand B toward the outside just enough to bring the side chain of Met64 within hydrogen bonding distance of residues present outside the β barrel. As the side chain of Met64 is locked in hydrogen bonding interactions, it introduces an anticlockwise twist in the strand B below and displaces part of the Ω loop located just above in a clockwise direction. These movements, especially the anticlockwise movement of strand B, pushes the side chain of Cys65 deeper inside the cavity, bringing the thiol group within hydrogen bonding distance of the endoperoxide oxygen of PGH_2. Thus, Met64 is essential for bring-

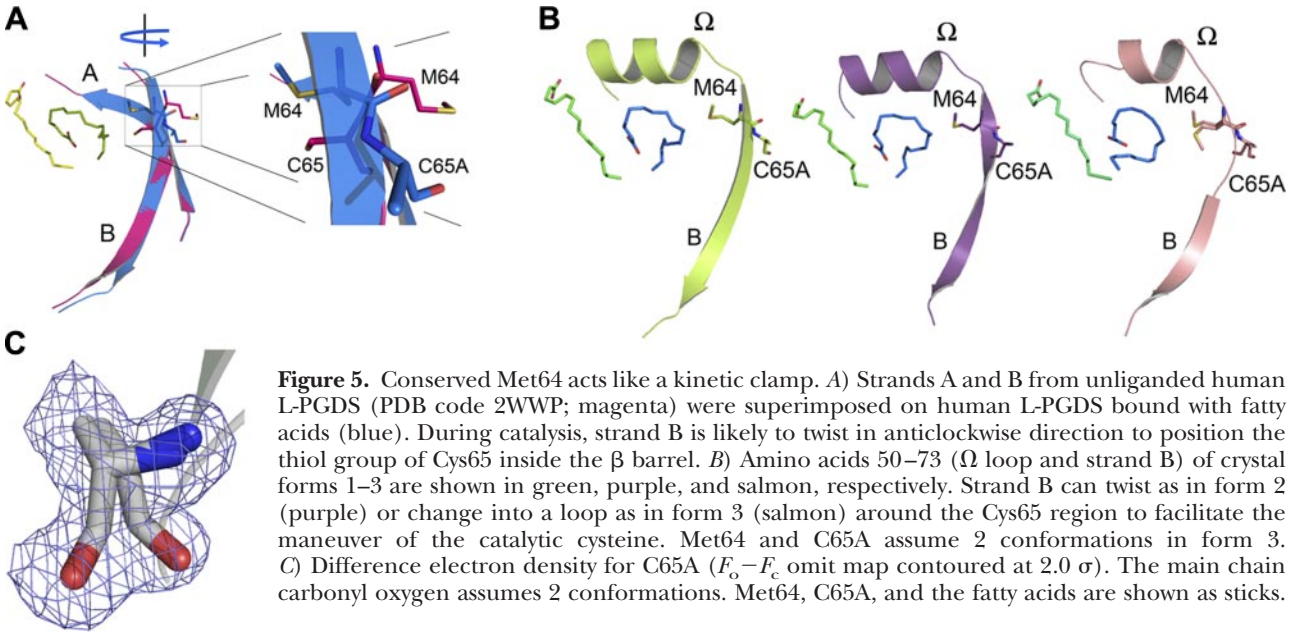

Figure 5. Conserved Met64 acts like a kinetic clamp. *A*) Strands A and B from unliganded human L-PGDS (PDB code 2WWP; magenta) were superimposed on human L-PGDS bound with fatty acids (blue). During catalysis, strand B is likely to twist in anticlockwise direction to position the thiol group of Cys65 inside the β barrel. *B*) Amino acids 50–73 (Ω loop and strand B) of crystal forms 1–3 are shown in green, purple, and salmon, respectively. Strand B can twist as in form 2 (purple) or change into a loop as in form 3 (salmon) around the Cys65 region to facilitate the maneuver of the catalytic cysteine. Met64 and C65A assume 2 conformations in form 3. *C*) Difference electron density for C65A (F_o-F_c omit map contoured at 2.0 σ). The main chain carbonyl oxygen assumes 2 conformations. Met64, C65A, and the fatty acids are shown as sticks.

ing the thiol group of Cys65 in proximity to the site of nucleophilic attack. Such a role for Met64 in catalysis is partly supported by an NMR study reported previously, which showed that among all the amino acids of mouse L-PGDS, backbone amides of Met64 and Cys65 displayed the largest chemical shift in presence of a PGH_2 analog, U-46619 (13). Met64 acts like a kinetic clamp with a role of introducing a twist, which not only helps push and position the putative catalytic nucleophile Cys65 inside the β barrel optimally, but in addition, the torsion force generated by the twist probably assists in product release. Our mutagenesis and kinetic data provide further evidence for this important role of Met64 in catalysis. The M64A mutant displayed a K_m of 32.5 μM and a V_{max} of 2.25 μmol/min/mg in comparison to the wild-type enzyme, which showed a K_m of 13.8 μM and a V_{max} of 9.27 μmol/min/mg protein when assayed under identical conditions. Although the reduction in V_{max} for M64A was very significant, the V_{max} values calculated at lower concentrations of the substrate generally tend to be inaccurate. Therefore, we assayed the M64A and wild-type enzyme at saturating concentrations of the substrate under identical conditions. The M64A mutant showed only 12% of the activity of that of the wild-type enzyme, underscoring the importance of Met64 in catalysis. Further, Met64 is absolutely conserved among all the orthologs of L-PGDS (Fig. 4), suggesting an evolutionary conserved role for Met64 in catalysis.

Finally, to obtain direct structural evidence that the region around Met64 and Cys65 is flexible, we looked at another structure of human L-PGDS at 1.4-Å resolution (Table 1) and compared the secondary structural elements of all 3 structures of human L-PGDS. The region surrounding the C65A mutation clearly showed the largest deviations (Fig. 5*B*), suggesting that this region is mobile. Strand B is shorter in the crystal form 3 (shown in salmon, Fig. 5*B*), when compared to the other 2 structures. Instead of Ser63, the strand begins from Lys66, and therefore C65A is now in a loop region. In the structure of the unliganded L-PGDS (PDB code 2WWP), Cys65 is located in a similar loop region (Fig. 5*A*). These observations seem to suggest that aa 63–65 can interchange between a strand and a loop to facilitate catalysis. Superimposition studies revealed that the main chain carbonyl oxygen of C65A assumes different conformations. The electron density was clear around this region and allowed unambiguous placement of residues. Further, the strained backbone geometry of C65A places it in the outliers of the Ramachandran plot, suggesting an unstable high-energy intermediate state of C65A trapped in the crystal structure. This is evident in the 1.4-Å resolution structure, where the main chain carbonyl oxygen assumes 2 conformations (Fig. 5*C*). Taken together, these results suggest that human L-PGDS is able to accomplish distinct tasks such as transport or enzymatic catalysis by either moving the side chain of Cys65 away from the cavity of the β barrel, such as during the transport of ligands such as fatty acids, or by swinging the side chain of Cys65 inside the cavity to convert PGH_2 to PGD_2. The ability of aa 63–65 to exist as either a strand or a loop and the twisting of the strand B are likely to assist in this maneuver of Cys65.

Insights into the mechanism of catalysis

The mode of binding of OLA and the results of the mutagenesis studies carried out on the residues in vicinity of OLA suggest that OLA potentially mimics the binding of the substrate PGH_2 to the enzyme. The lengths of OLA and PGH_2 measured from the carboxyl group to the ω carbon are almost similar, with PGH_2 being marginally shorter in length by 1 carbon atom. The endoperoxide

nucleus of PGH_2 would be placed between C8-C9 atoms of the OLA if the mode of binding of OLA is similar to that of PGH_2. This would position the pentane ring opposite to Phe83. A greater than 80% decrease in the catalytic efficiency of the F83A mutation partly supports such a position for the endoperoxide group (Table 2). More important, such a position places the endoperoxide oxygen of C11 within hydrogen bonding distance of the thiol group of the catalytically critical Cys65. Analysis of the structure suggests that the positions of Wat48 and Wat99 are unlikely to be affected by the placement of the endoperoxide group, implicating a role for these waters in catalysis. The thiol group of Cys65 forms a 2.9- and a 2.5-Å hydrogen bond with Wat48 and Wat99, respectively, when the structure of unliganded L-PGDS (PDB code 2WWP) was superimposed over our structure (Fig. 3*D*). Wat48 is linked to Wat99 *via* a 2.85-Å hydrogen bond. Further, Wat48 sits in the center of a triangular pocket formed by Ser45, Ser67 and the thiol group of Cys65 (Figs. 3*C, D*). This arrangement suggests that the thiol group of Cys65 on activation by Ser45, Ser67, and possibly Wat48 and Wat99 is likely to mount a nucleophilic attack at C11 of PGH_2. Alternatively, one cannot rule out the possibility of Wat99, activated by the thiolate group of Cys65 acting as a nucleophile. Previously, using docking, mutagenesis and thiol modification studies on mouse L-PGDS, Ser45, Thr67 (Ser67 in humans), and Ser81 have been proposed to activate the thiol group of Cys65, which mounts a nucleophilic attack on the endoperoxide oxygen. The formation of the carbonyl group is accomplished by Cys65 abstracting a proton from C11 (14). Our structure of human L-PGDS bound with ligands suggests a role for water molecules in the catalysis of PGH_2. Particularly, the hydrogen bonding network of Wat48 and Wat99 seems to be important for the relay of charge and catalysis. However, a structure of the L-PGDS in complex with PGH_2 is required to unravel the exact mechanism of catalysis.

Lipocalin fold confers functional versatility

The structural flexibility of the lipocalin fold of human L-PGDS helps explain its promiscuity in ligand binding. Human L-PGDS is able to bind ligands of various sizes and shapes by altering the orientation of the strands and conformational rearrangement of the loop regions. Tear lipocalin has been shown to bind various natural and artificial ligands using such a mechanism (24). However, one question that arises is why do humans employ such a promiscuous enzyme with a lipocalin fold to metabolize prostonoids?

Arachidonic acid (ARA) is an "essential fatty acid," important for the development of neurons (25). It helps maintain membrane fluidity and protects the brain from oxidative stress (26). In addition to ARA, eicosapentaenoic acid (EPA) and dihomo-γ-linolenic acid (DGLA) are found in the cell membrane and are released by the action of phospholipases during inflammation (27). Once released, these fatty acids can be metabolized to eicosonoids, which are known to modulate the inflammatory response (28). Eicosonoids derived from ARA are proinflammatory, whereas eicosonoids synthesized from EPA and DGLA are anti-inflammatory (29). Since ARA, EPA, and DGLA compete with each other for the cyclooxygenase and lipooxygenase necessary for the production of eicosonoids, the inflammatory response can be moderated by increasing the concentration of EPA and DGLA (30). Humans procure ARA directly from the diet or can synthesize it from dietary linoleic acid by the action of elongase and desaturase (31). Similarly, EPA and DGLA are synthesized from α-linolenic acid using elongase and desaturase. However, α-linolenic acid has a higher affinity for these enzymes and can displace the linoleic acid from the enzyme, thereby lowering the production of ARA (32). Is it likely, then, that L-PGDS, in its role as a lipocalin, sequesters linoleic and α-linolenic acid to regulate the synthesis of ARA, EFA, and DGLA? Further, the mode of binding of fatty acids suggests that the lipocalin fold of L-PGDS can potentially bind 2 molecules of PGH_2 and prevent the rearrangement of PGH_2 to levuglandins by rapidly removing PGH_2 from circulation. Levuglandins have been shown to form covalent adducts with proteins causing their aggregation, resulting in numerous physiological changes detrimental to the cells (33).

In the structure of human L-PGDS described here, OLA binds in proximity of the catalytically essential Cys65, possibly mimicking the binding of the substrate PGH_2. The aliphatic chain of OLA encircles the amine nitrogen of Lys59. Such a mode of ligand binding involving Lys59 has not been speculated by numerous modeling, mutagenesis, and functional studies reported before for mouse L-PGDS. Further, Lys59 is absolutely conserved among all the orthologs of L-PGDS. Without the structure of the L-PGDS in complex with the fatty acids reported here, it would not have been possible to envision a role for this conserved amino acid in ligand binding, underscoring the importance of enzyme-ligand complexes in mechanistic interpretations.

Although several lines of evidence suggest that Cys65 is highly mobile, the orientation of the C65A mutation observed in our structure (facing outside the cavity of the β barrel) remains unexplained. The question of whether such a conformation displayed by the C65A is merely due to an artifact introduced by the mutation or a result of the binding of the fatty acids remains unanswered. A complete understanding of the detailed mechanism will require the structures of the binary complexes of the wild-type human L-PGDS with fatty acids and its substrate PGH_2.

In summary, the structures of human L-PGDS in complex with fatty acids described here provide for the first time the structural basis for ligand binding in L-PGDS. Based on the structure of the fatty acid bound human L-PGDS, amino acids important for the catalysis of L-PGDS have been identified by site-directed mutagenesis and kinetic analysis. Our studies suggest a role for water molecules in catalysis. More important, we have mapped the location of water molecules, which is

an important consideration during mechanistic interpretations and optimization of lead compounds. The structure-function analysis data reported here open up new opportunities for designing small molecules to modulate the activity of L-PGDS. FJ

This work was funded by the Ministry of Science and Technology of China (grants 2006AA02A316, 2009DFB30310, and 2006CB910901), the National Natural Science Foundation of China (grants 30670427 and 30721003), the Ministry of Health of China (grant 2008ZX10404), a CAS research grant (KSCX2-YW-R-127 and INFO-115-D01-2009), and a CAS fellowship for young international scientists (grant 2010Y1SA1) awarded to N.S. Crystallographic data were collected at beamline BL17U1 of the SSRF (Shanghai, China).

REFERENCES

1. Urade, Y., and Hayaishi, O. (2000) Prostaglandin D synthase: structure and function. *Vitam. Horm.* **58,** 89–120
2. Pettipher, R., Hansel, T. T., and Armer, R. (2007) Antagonism of the prostaglandin D2 receptors DP1 and CRTH2 as an approach to treat allergic diseases. *Nat. Rev. Drug Discov.* **6,** 313–325
3. Qu, W.-M., Huang, Z.-L., Xu, X.-H., Aritake, K., Eguchi, N., Nambu, F., Narumiya, S., Urade, Y., and Hayaishi, O. (2006) Lipocalin-type prostaglandin D synthase produces prostaglandin D2 involved in regulation of physiological sleep. *Proc. Natl. Acad. Sci. U. S. A.* **103,** 17949–17954
4. Eguchi, N., Minami, T., Shirafuji, N., Kanaoka, Y., Tanaka, T., Nagata, A., Yoshida, N., Urade, Y., Ito, S., and Hayaishi, O. (1999) Lack of tactile pain (allodynia) in lipocalin-type prostaglandin D synthase-deficient mice. *Proc. Natl. Acad. Sci. U. S. A.* **96,** 726–730
5. Malki, S., Nef, S., Notarnicola, C., Thevenet, L., Gasca, P., Mejean, C., Berta, P., Poulat, F., and Boizet-Bonhoure, B. (2005) Prostaglandin D2 induces nuclear import of the sex-determining factor SOX9 via its cAMP-PKA phosphorylation. *EMBO J.* **24,** 1798–1809
6. Kanaoka, Y., Ago, H., Inagaki, E., Nanayama, T., Miyano, M., Kikuno, R., Fujii, Y., Eguchi, N., Toh, H., Urade, Y., and Hayaishi, O. (1997) Cloning and crystal structure of hematopoietic prostaglandin D synthase. *Cell* **90,** 1085–1095
7. Urade, Y., and Hayaishi, O. (2000) Biochemical, structural, genetic, physiological, and pathophysiological features of lipocalin-type prostaglandin D synthase. *Biochim. Biophys. Acta* **1482,** 259–271
8. Hoffmann, A., Conradt, H. S., Gross, G., Nimtz, M., Lottspeich, F., and Wurster, U. (1993) Purification and chemical characterization of beta-trace protein from human cerebrospinal fluid: its identification as prostaglandin-D synthase. *J. Neurochem.* **61,** 451–456
9. Tanaka, T., Urade, Y., Kimura, H., Eguchi, N., Nishikawa, A., and Hayaishi, O. (1997) Lipocalin-type prostaglandin D synthase (β-trace) is a newly recognized type of retinoid transporter. *J. Biol. Chem.* **272,** 15789–15795
10. Beuckmann, C. T., Aoyagi, M., Okazaki, I., Hiroike, T., Toh, H., Hayaishi, O., and Urade, Y. (1999) Binding of biliverdin, bilirubin, and thyroid hormones to lipocalin-type prostaglandin D synthase. *Biochemistry* **38,** 8006–8013
11. Hansson, S. F., Andréasson, U., Wall, M., Skoog, I., Andreasen, N., Wallin, A., Zetterberg, H., and Blennow, K. (2009) Reduced levels of amyloid-β-binding proteins in cerebrospinal fluid from Alzheimer's disease patients. *J. Alzheimer's Dis.* **16,** 389–397
12. Mohri, I., Taniike, M., Okazaki, I., Kagitani-Shimono, K., Aritake, K., Kanekiyo, T., Yagi, T., Takikita, S., Kim, H. S., Urade, Y., and Suzuki, K. (2006) Lipocalin-type prostaglandin D synthase is up-regulated in oligodendrocytes in lysosomal storage diseases and binds gangliosides. *J. Neurochem.* **97,** 641–651
13. Shimamoto, S., Yoshida, T., Inui, T., Gohda, K., Kobayashi, Y., Fujimori, K., Tsurumura, T., Aritake, K., Urade, Y., and Ohkubo, T. (2007) NMR solution structure of lipocalin-type prostaglandin D synthase. *J. Biol. Chem.* **282,** 31373–31379
14. Kumasaka, T., Aritake, K., Ago, H., Irikura, D., Tsurumura, T., Yamamoto, M., Miyano, M., Urade, Y., and Hayaishi, O. (2009) Structural basis of the catalytic mechanism operating in open-closed conformers of lipocalin type prostaglandin D synthase. *J. Biol. Chem.* **284,** 22344–22352
15. Stols, L., Gu, M., Dieckman, L., Raffen, R., Collart, F. R., and Donnelly, M. I. (2002) A new vector for high-throughput, ligation-independent cloning encoding a tobacco etch virus protease cleavage site. *Protein Expr. Purif.* **25,** 8–15
16. Vagin, A., and Teplyakov, A. (1997) MOLREP: an automated program for molecular replacement. *J. Appl. Crystallogr.* **30,** 1022–1025
17. Terwilliger, T. C., Grosse-Kunstleve, R. W., Afonine, P. V., Moriarty, N. W., Zwart, P. H., Hung, L.-W., Read, R. J., and Adams, P. D. (2008) Iterative model building, structure refinement and density modification with the PHENIX AutoBuild wizard. *Acta Crystallogr. D* **64,** 61–69
18. Emsley, P., and Cowtan, K. (2004) Coot: model-building tools for molecular graphics. *Acta Crystallogr. D* **60,** 2126–2132
19. Murshudov, G. N., Vagin, A. A., and Dodson, E. J. (1997) Refinement of macromolecular structures by the maximum-likelihood method. *Acta Crystallogr. D* **53,** 240–255
20. Davis, I. W., Leaver-Fay, A., Chen, V. B., Block, J. N., Kapral, G. J., Wang, X., Murray, L. W., Arendall, W. B., III, Snoeyink, J., Richardson, J. S., and Richardson, D. C. (2007) MolProbity: all-atom contacts and structure validation for proteins and nucleic acids. *Nucleic Acids Res.* **35,** W375–W383
21. Altschul, S. F., Madden, T. L., Schaffer, A. A., Zhang, J., Zhang, Z., Miller, W., and Lipman, D. J. (1997) Gapped BLAST and PSI-BLAST: a new generation of protein database search programs. *Nucleic Acids Res.* **25,** 3389–3402
22. Irikura, D., Kumasaka, T., Yamamoto, M., Ago, H., Miyano, M., Kubata, K. B., Sakai, H., Hayaishi, O., and Urade, Y. (2003) Cloning, expression, crystallization, and preliminary X-ray analysis of recombinant mouse lipocalin-type prostaglandin D synthase, a somnogen-producing enzyme. *J. Biochem.* **133,** 29–32
23. Fujimori, K., Inui, T., Uodome, N., Kadoyama, K., Aritake, K., and Urade, Y. (2006) Zebrafish and chicken lipocalin-type prostaglandin D synthase homologues: conservation of mammalian gene structure and binding ability for lipophilic molecules, and difference in expression profile and enzyme activity. *Gene* **375,** 14–25
24. Breustedt, D. A., Chatwell, L., and Skerra, A. (2009) A new crystal form of human tear lipocalin reveals high flexibility in the loop region and induced fit in the ligand cavity. *Acta Crystallogr. D* **65,** 1118–1125
25. Darios, F., and Davletov, B. (2006) Omega-3 and omega-6 fatty acids stimulate cell membrane expansion by acting on syntax-in[thinsp]3. *Nature* **440,** 813–817
26. Wang, Z.-J., Liang, C.-L., Li, G.-M., Yu, C.-Y., and Yin, M. (2006) Neuroprotective effects of arachidonic acid against oxidative stress on rat hippocampal slices. *Chemico-Biol. Interact.* **163,** 207–217
27. Kaiser, E. (1999) Phospholipase A2: its usefulness in laboratory diagnostics. *Crit Rev. Clin. Lab. Sci.* **36,** 65–163
28. Calder, P. C. (2006) n-3 Polyunsaturated fatty acids, inflammation, and inflammatory diseases. *Am. J. Clin. Nutr.* **83,** S1505–1519
29. Tilley, S. L., Coffman, T. M., and Koller, B. H. (2001) Mixed messages: modulation of inflammation and immune responses by prostaglandins and thromboxanes. *J. Clin. Invest.* **108,** 15–23
30. Das, U. N. (2006) Essential fatty acids: a review. *Curr. Pharm. Bio/Technol.* **7,** 467–482
31. Needleman, P., Truk, J., Jakschik, B. A., Morrison, A. R., and Lefkowith, J. B. (1986) Arachidonic acid metabolism. *Annu. Rev. Biochem.* **55,** 69–102
32. Phinney, S. D., Odin, R. S., Johnson, S. B., and Holman, R. T. (1990) Reduced arachidonate in serum phospholipids and cholesteryl esters associated with vegetarian diets in humans. *Am. J. Clin. Nutr.* **51,** 385–392
33. Salomon, R. G., Kaur, K., and Batyreva, E. (2000) Isolevuglandin-protein adducts in oxidized low density lipoprotein and human plasma: a strong connection with cardiovascular disease. *Trends Cardiovasc. Med.* **10,** 53–59

Received for publication May 21, 2010.
Accepted for publication July 15, 2010.